Nontrivial Differentiation between Two Identical Functionalities within the Same Molecule Studied by STM

Steven De Feyter,[†] Petrus C. M. Grim,[†] Jan van Esch,[‡] Richard M. Kellogg,[‡] Ben L. Feringa,[‡] and Frans C. De Schryver*[,†]

Department of Chemistry, Laboratory of Molecular Dynamics and Spectroscopy, University of Leuven (KULeuven), Celestijnenlaan 200-F, 3001 Heverlee, Belgium, and Department of Organic and Molecular Inorganic Chemistry, University of Groningen, Nijenborgh 4, 9747 AG, Groningen, The Netherlands

Received: September 30, 1997; In Final Form: May 28, 1998

Physisorbed monolayer films of small alkyl-substituted bisurea derivatives based on the structure $R_1-NHCONH-R_2-NHCONH-R_1$ with $R_1 = C_{12}H_{25}$ and $R_2 = C_9H_{18}$ or $C_{12}H_{24}$ have been imaged on graphite (HOPG) at the solution−substrate interface using scanning tunneling microcopy (STM). They form well-ordered two-dimensional monolayers, which are imaged with submolecular resolution. The number of carbon atoms (odd or even) in the alkyl spacer between both urea groups determines the molecular conformation giving rise to an odd−even effect. The nonlinear conformation of these molecules could easily be visualized in the STM images. The position of the urea moieties can clearly be assigned. Lamellae of these compounds are remarkably stable, which allows for study of monolayer defects in detail. Surprisingly, sometimes urea groups reveal contrast variation within a monolayer. For $R_2 = C_{12}H_{24}$, the contrast of the urea groups differs within one molecule. On the other hand, the contrast of both urea groups for $R_2 = C_9H_{18}$ is the same within a molecule, but also for this compound, contrast variation is observed within a monolayer. For both compounds, this contrast variation is correlated with the orientation of the molecules within the monolayer.

Introduction

Scanning tunneling microscopy (STM) has proven to be a powerful tool in studying physisorbed adlayers of organic molecules on atomically flat conductive surfaces among which graphite is the most popular one. Since the pioneering experiments on physisorbed monolayers of normal alkanes[1,3] and alcohols[2,3] on graphite by STM, considerable knowledge has been acquired on the forces that rule the two-dimensional packing of alkyl-substituted molecules. Both adsorbate−adsorbate and adsorbate−substrate interactions control the ordering of these physisorbed monolayers. In most cases, adsorbed alkanes and alkyl groups tend to adopt an all-trans conformation with their molecular axis parallel to the graphite substrate and in line with one of graphite's main symmetry axes, confirming the influence of the graphite substrate on the two-dimensional organization of those molecules. The molecules lie in rows parallel to each other in order to optimize the energetics of the intermolecular and molecule−substrate interactions. Normal alkanes[1,3,4,5] adopt a 90° orientation with respect to the lamellar axis. This holds also for a number of terminally substituted hydrocarbons such as 1-chlorooctadecane ($CH_3(CH_2)_{17}Cl$), 1-bromodocesane ($CH_3(CH_2)_{21}Br$), and 1-iodooctane ($CH_3(CH_2)_{17}I$).[6] Terminally substituted monoalcohols[2,3,4,7] and monoamines[6] are oriented with their molecular axis at an angle of 60° with the direction of the lamellar axis in order to allow for optimal hydrogen bonding between molecules in adjacent lamellae. Terminally substituted monosulfides,[4] which in principle are capable of forming weak hydrogen bonds, are however oriented with their molecular axis at an angle of 90° with the direction of the lamellar axis. Moreover, the sulfide groups are not lined up within a lamella as found for other terminally monosubstituted hydrocarbons, and the sulfide groups of molecules in adjacent lamellae do not necessarily adopt a head-to-head arrangement, indicating that hydrogen bonding does not play a major role in the ordering of the molecules during the formation of the monolayer. Terminally substituted carboxylic acids do adopt a 90° orientation with respect to the lamellar axis, but this orientation allows for optimal hydrogen bonding between molecules in adjacent lamellae.[3,8]

Another important aspect of the investigation of organic adlayers with STM is its ability to distinguish certain functional groups from the alkyl groups. The tunneling current between the graphite surface and the STM tip is influenced by the physisorbed monolayer under the experimental conditions applied to image this monolayer. There are several theories describing the origin of the STM contrast. One theory proposes a model in which the adsorbate image contrast is ruled by its contribution to the local density of states (LDOS) at the Fermi level of the substrate.[9] Other groups have proposed that the molecular states themselves are directly involved as intermediates in the tunneling process.[10,11,12] In another theory, the image contrast is governed by the extent to which the surface work function is influenced by the adsorbate.[13] The relative brightness (the brighter, the higher the tunneling current) may change for different functional groups. Since the pioneering STM work on liquid crystals,[14] it is known that aromatic moieties appear much brighter in the STM image than the alkyl chains. Cyr et al.[6] investigated the relative contrast of functional groups of terminally substituted hydrocarbons (CH_3, OH, Cl, NH_2, SH, Br, I) in physisorbed monolayers. The SH, I, Br, and NH_2 end groups appeared as bright spots in the STM image, and the relative brightness with respect to the remainder of the alkyl

* To whom correspondence should be addressed.
[†] University of Leuven.
[‡] University of Groningen.

10.1021/jp973177x CCC: $15.00
Published on Web 10/16/1998

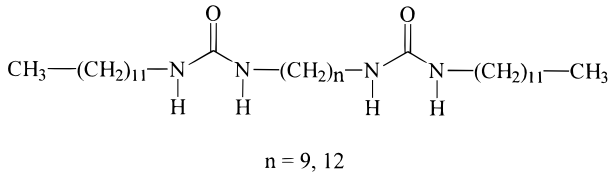

Figure 1. Chemical structure of $C_{12}-U-C_n-U-C_{12}$.

chain increased from NH_2 to SH in the following way: NH_2 < Br < I < SH. On the other hand, the CH_3, OH, and Cl end groups could not be distinguished from the remainder of the alkyl chain. Cyr et al. compared the relative contrast of those functional groups with their polarizability and found that the relative brightness increased with the polarizability of those functional groups, with the exception of SH. They also found some tendencies that are in correspondence with the theory proposed by Lang et al.:[9] any feature of the adsorbate that pushes the spatial extent of its electronic wave function farther above the surface will enhance the tunneling current associated with the adsorbate or specific functional groups of the adsorbate. The difference in relative brightness of the functional groups is promising as it provides a possible tool to differentiate unlike functional groups within the same STM image or even within the same molecule. Recently, Claypool et al.[15] investigated a series of functionalized alkanes. The STM contrast produced by the various functional groups was found to be dominated by variations in local electronic coupling. They have shown that, on the basis of the HOMO-derived electronic coupling term estimated from the ionization potential, compounds with a lower ionization potential than methylene groups appear brighter in the STM image than those methylene groups. On the basis of these observations, Faglioni et al.[16] have developed a theoretical model describing the STM images of alkanes and substituted alkanes adsorbed on graphite based upon perturbation theory.

So far, the major part of STM studies on functionalized "small" alkyl-substituted organic materials that are physisorbed at the liquid−graphite interface have dealt with hydrocarbons that are terminally substituted.[17] A few reports appeared in which the reactivity of organic compounds was studied on the molecular scale with STM. The cis−trans isomerization of an azobenzene-containing isophthalic acid derivative,[18] as well as the photopolymerization of a diacetylene-containing isophthalic acid derivative,[19] was reported. In this paper, we have investigated the order in two-dimensional films of alkyl-substituted bisurea ($R_1-NHCONH-R_2-NHCONH-R_1$) derivatives. To determine the effect of the length of the alkyl spacer and to check the existence of an odd−even effect in the conformation of the molecules, two bisurea derivatives that differ from each other in the number of carbon atoms of the alkyl spacer are studied. The compounds under investigation are 1-dodecyl-3-[9-(3-dodecylureido)nonyl]urea ($C_{12}-U-C_9-U-C_{12}$) ($R_1 = 12$, $R_2 = 9$) and 1-dodecyl-3-[12-(3-dodecylureido)dodecyl]urea ($C_{12}-U-C_{12}-U-C_{12}$) ($R_1 = 12$, $R_2 = 12$). The chemical structure of these compounds is depicted in Figure 1.

Another point of interest is also the image contrast provided by the urea groups. Would it be possible to localize the position of the urea functionalities in the STM images and, if so, to distinguish between both urea groups within the same molecule? A step beyond the ability to identify the position of two similar functionalities is the capability to determine the orientation of a functional group within a molecule by means of deduction based on the apparent conformation of a molecule in a monolayer or, more interestingly, by means of the contrast provided by the functional groups themselves.

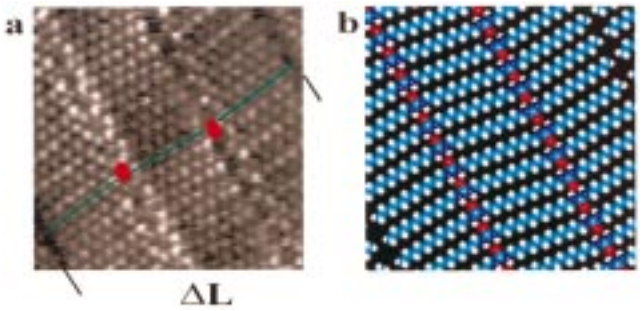

Figure 2. STM image of an ordered monolayer of $C_{12}-U-C_{12}-U-C_{12}$ molecules formed by physisorption from 1-octanol at the liquid−graphite interface. (a) Image size is 4.6 × 4.6 nm^2. Tunneling current and voltage are 0.5 nA and −0.35 V, respectively. ΔL is the width of one lamella. The orientation of a molecule is indicated by a stick model. The urea groups are represented by red ovals, which also indicate the direction of the carbonyl groups. (b) Molecular model for the two-dimensional packing of $C_{12}-U-C_{12}-U-C_{12}$ molecules corresponding with the monolayer presented in (a).

Experimental Section

The synthesis of $C_{12}-U-C_9-U-C_{12}$ and $C_{12}-U-C_{12}-U-C_{12}$ was reported previously.[20]

Prior to STM experiments, the compounds under investigation were dissolved in 1-octanol (Sigma, 99.6%) and the solution was heated until a clear solution was obtained. Solvents such as 1-phenyloctane and 1,2,4-trichlorobenzene, classically used in STM microscopy, are not useful as many of the urea derivatives form a gel on cooling in these solvents. 1-Octanol seemed to be an appropriate solvent as it competes for hydrogen bonding with the solute molecules. Concentrations used were typically ∼1 mg/mL. Samples were prepared by spreading a drop of the solution on the basal plane of highly ordered pyrolytic graphite (HOPG) (grade ZYB, Advanced Ceramics Inc., Cleveland, OH).

The STM images were acquired in the variable-current mode (constant height) under ambient conditions. STM images obtained at low bias voltages reliably revealed the atomic structure of HOPG, providing an internal calibration standard for each obtained image. STM experiments were performed using a Discoverer scanning tunneling microscope (Topometrix Inc., Santa Barbara, CA) and an external pulse/function generator (model HP 8111 A). Tips were electrochemically etched from Pt/Ir wire (80%/20%, diameter 0.2 mm) in 2 N KOH/6 N NaCN solution in water. Typically, a tunneling current of 0.4−1 nA and a bias voltage of 0.4−0.7 V (sample negative) were employed when the monolayers were imaged. The STM data presented were not subjected to image processing.

All molecular models presenting monolayer structures are assembled and based upon the structural parameters (distances and angles) derived from the STM image, based on the observed Moiré pattern (vide infra) and the above-mentioned calibration. In the molecular models, carbon atoms appear light blue, nitrogen atoms are dark blue, oxygen atoms are red, and hydrogen atoms are white.

Results and Discussion

Bisurea Derivatives. Figure 2a is a STM image of an ordered monolayer of $C_{12}-U-C_{12}-U-C_{12}$ molecules adsorbed from a 1-octanol solution of $C_{12}-U-C_{12}-U-C_{12}$ applied to the basal plane of HOPG. This image reveals a closely packed

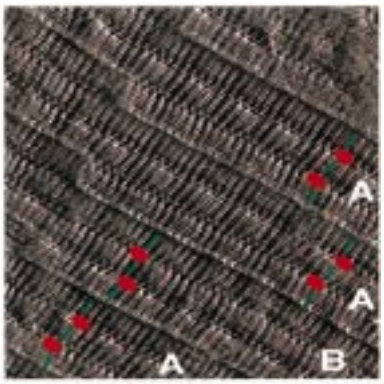

Figure 3. STM image of an ordered monolayer of $C_{12}-U-C_{12}-U-C_{12}$ molecules formed by physisorption from 1-octanol at the liquid−graphite interface. Image size is 18.5×18.5 nm^2. Tunneling current and voltage are 1.0 nA and −2.0 V, respectively. A and B in the image represent the two different lamellar types, based upon the orientation of the molecules within the lamellae. The orientation of some molecules is indicated by a stick model.

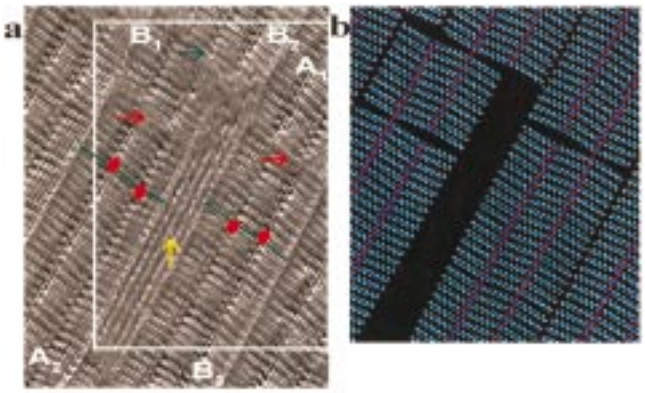

Figure 4. (a) STM image of an ordered monolayer of $C_{12}-U-C_{12}-U-C_{12}$ molecules formed by physisorption from 1-octanol at the liquid−graphite interface. Image size is 13.6×17.2 nm^2. Tunneling current and voltage are 1.0 nA and −0.20 V, respectively. A and B in the image represent the two different lamellar types, based upon the orientation of the molecules within the lamellae. The subscript corresponds with a lamella or lamellar part. The orientation of some molecules is indicated by a stick model. The green arrow indicates a defect where one lamella is translated one-third of the lamellar width in a direction perpendicular to the lamellar axis with respect to the other lamella. The red arrow indicates a defect where molecules adopt a different orientation within the same row of molecules. The yellow arrow indicates the defect area. (b) Molecular model for the two-dimensional packing of $C_{12}-U-C_{12}-U-C_{12}$ molecules corresponding with the indicated area of the monolayer presented in (a).

arrangement of molecules on the graphite substrate with submolecular resolution. The urea groups can be distinguished from the remainder of the molecules. They are lined up and appear as two parallel rows within a lamella. Lamellae are separated from each other by small dark lines. The alkyl chains are clearly visible and their orientation can easily be assigned. The alkyl spacer between both urea moieties makes an angle of 3−5° with the outermost alkyl chains of the molecule, which are lying parallel to each other. The apparent conformation of a single molecule within the STM image can easily be correlated with the shape of a molecular model, which permits the orientation of the molecules on the graphite surface, including the orientation of the urea groups, to be determined. Therefore, carbonyl groups of the left row of urea groups point to the upper side of the image, and the carbonyl groups of the right row of urea groups point to the lower side of the image. A stick model indicates the orientation of a molecule. The urea groups are represented by red ovals, which also indicate the direction of the carbonyl groups. Molecules within a lamella form hydrogen bonds with their nearest neighbors as the molecules within a lamella adopt the same orientation and as the intermolecular distance measures 0.462 ± 0.010 nm.[21] Further support for the formation of hydrogen bonding is found in the stability of lamellae, which will be discussed below. One could argue that the conformation of the molecules determines the packing of the molecules within the lamellae and that hydrogen bonding stabilizes this packing. The lamellar width is 5.4 ± 0.1 nm. Figure 2b represents a molecular model for the STM image given in Figure 2a.

Figure 3 is a larger scale STM image of an ordered monolayer formed by $C_{12}-U-C_{12}-U-C_{12}$ from a 1-octanol solution on the basal plane of HOPG. Lamellae and individual molecules are visible with submolecular resolution. The position of urea groups and alkyl chains and the molecular conformation can easily be determined in the STM image due to the small angle between the alkyl spacer and the outermost alkyl chains. Furthermore, the contrast of the urea groups differs for both rows of urea groups within the same lamella. The contrast, formed by the sequence of dark and bright spots, is more pronounced for one row of urea moieties, which allows both to be easily distinguished. A stick model indicates the orientation of the molecules in each lamella. The lamellae in the upper left part of the image are shifted in a direction perpendicular to the lamellar axes by one-third of the lamellar width with respect to the lamellae in the rest of the image. Molecules in adjacent lamellae can adopt two different orientations, determining the lamellar type, denoted in the STM image as A or B. Those different lamellar types cannot be superimposed by any rotation or translation of lamellae in a plane parallel to the graphite surface. Both lamellar types coexist in a random way. The orientation of molecules in one lamella is not influenced by the orientation of molecules in adjacent lamellae. It is clear that the apparent molecular conformation in the STM images determines the position and the orientation of the molecules and their functional groups. The difference in contrast between both rows of urea groups within the same lamella indicates that the orientation of the urea groups in both rows is different. This effect is likely due to tip−adsorbate interactions (vide infra).

STM images also reveal other interesting structural properties of monolayers composed of $C_{12}-U-C_{12}-U-C_{12}$ molecules. As already mentioned in Figure 3, some defects can arise in the monolayers. In Figure 3, lamellae in the upper left part of the image are shifted one-third of the lamellar width in a direction perpendicular to the lamellar axes. Figure 4a is a STM image of a monolayer built up of $C_{12}-U-C_{12}-U-C_{12}$ molecules, which contains a number of different defects that are typical for monolayers built up by $C_{12}-U-C_{12}-U-C_{12}$. As in the other images, the position of the urea groups, the difference in contrast of the urea groups within one lamella, the molecular conformation, and consequently the orientation of the urea groups can easily be determined in this image. Some stick models are drawn that indicate the orientation of the molecules in different parts of the monolayer. For convenience, the different lamellae, parts of lamellae, or defects are labeled in the STM image. The two different lamellar types, which are determined by the orientation of the molecules within the respective lamellae, are denoted as A and B. The subscript refers to a lamella or lamellar part. Colored arrows indicate different defect types. A defect similar to that found in Figure 3 is indicated by a green arrow. Lamellar parts B_1 and B_2 are shifted one-third of the lamellar width with respect to each other. When this shift occurs between lamellar parts of the same type,

the hydrogen-bonding pattern is not continued at the defect site from one urea row in one lamellar part to another urea row in the other lamellar part, which is also demonstrated in the molecular model given in Figure 4b. Another defect, indicated by a red arrow, is given at the boundary between A_1 and B_3 and at the boundary between B_1 and A_2. Within the same row of molecules, two different types of orientation can be distinguished. This change in orientation of the molecules within the same row can clearly be recognized by the change in contrast of the urea groups and the mirror-shaped appearance of the molecules in adjacent but different lamellar parts. It is obvious that the conformation of the molecules dominates the molecular ordering within the lamellae, neglecting the hydrogen bond formation. However, hydrogen bonding will stabilize the molecular ordering and will allow imaging these defects with great detail. A yellow arrow indicates a third defect, which is really a defect area. Within the defect area, four parallel lines are visible which are in line with the lamellar axes of the adjacent lamellae but perpendicular to one of the main axes of the graphite substrate underneath. This defect type is quite common for monolayers composed of $C_{12}-U-C_{12}-U-C_{12}$. The width of the defect area is one-third of the lamellar width, but in general, defects are found whose width is one- or two-thirds of the lamellar width. The length of these defect areas is variable. These defect areas contain 3−4 or 6−7 parallel lines, depending on the width of the defect area. The question arises as to how these originate. As already mentioned, all the lamellae in the upper left part of Figure 3 are shifted by one-third of the lamellar width with respect to the lamellae in the other part of the image. However, imagine that only a few lamellae would be translated. This would create a gap, which is the case in the monolayer presented in Figure 4a. As this is a two-component system, containing bisurea and 1-octanol molecules, the defect area could be occupied by one of them. A first possibility is that 1-octanol molecules fill up the defect area. Coadsorption of 1-octanol or 1-undecanol molecules in two-component systems has already been demonstrated in systems studied by Vanoppen et al.[18] and Grim et al.,[19] where lamellae of solvent molecules are coadsorbed in an alternating fashion with lamellae composed of isophthalic acid derivatives. The coadsorbed solvent molecules, which in most cases were imaged with submolecular resolution, were in general not in registry with the graphite surface underneath but stabilized by hydrogen bonding with the carboxylic acid functions of the isophthalic acid moieties. It is, however, unlikely that 1-octanol molecules will fill up the defect area. The existence of lines in the defect area perpendicular to one of the main symmetry axes in the graphite surface underneath suggests that the molecules in that area are adsorbed with their alkyl chains perpendicular to one of the substrate's symmetry axes. This orientation is not energetically favorable for the solvent molecules, as no optimal intermolecular hydrogen bonding between 1-octanol molecules or hydrogen bonding with bisurea molecules in adjacent lamellae can occur. It is suggested that this region is probably filled up by $C_{12}-U-C_{12}-U-C_{12}$ molecules. Indeed, the width of the defect area is large enough to accommodate the adsorption of 3−4 or 6−7 $C_{12}-U-C_{12}-U-C_{12}$ molecules, depending on the width of the defect. The distance between two lines varies from 4.2 to 4.4 Å. In general, the resolution of the features in these defect areas is poor. This is probably due to enhanced dynamics. The width of these defects is confined but not their length. This allows for some lateral motion of the adsorbed species along the defect length.

Another striking feature is the stability of lamellae composed of $C_{12}-U-C_{12}-U-C_{12}$ molecules. Stability in this context means that monolayers, single lamellae, and some features can be imaged with very high resolution. In some of the images shown, structural details could be imaged with high resolution also at monolayer defects. Figure 5 contains STM images of $C_{12}-U-C_{12}-U-C_{12}$ that represent some features demonstrating the astonishing stability of this system. From the lower left corner to the upper right corner of Figure 5a, a single lamella is visible. This lamella has no parallel adjacent lamellae as neighbors. Although this lamella is not embedded in a "matrix" of analogous lamellae, the molecules and their orientation can still be recognized with submolecular resolution. This suggests that hydrogen bonding, in addition to van der Waals interactions, plays a key role in the stabilization of the lamellae. Those stabilizing forces probably prevent a high exchange rate with the molecules in the bulk. After a few minutes, a second lamella is formed adjacent to the first one, and they bridge the "empty" graphite space between two large domains (image not shown). Another example that demonstrates the stability of this system is given in Figure 5b. In the center of the image, lamellar boundaries are visible of three lamellae with different orientation that meet each other and an "empty" triangle is formed. The lamellar boundaries are well resolved. The conformation of the molecules can easily be determined, and the difference in contrast of the urea groups is very clear.

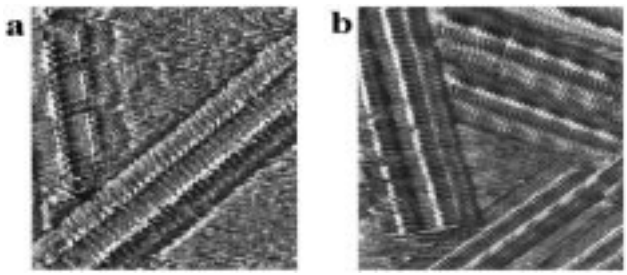

Figure 5. STM images of an ordered monolayer of $C_{12}-U-C_{12}-U-C_{12}$ molecules formed by physisorption from 1-octanol at the liquid−graphite interface. (a) A single lamella is visible which is surrounded by the graphite substrate. Image size is 14.1×14.1 nm^2. Tunneling current and voltage are 0.6 nA and −0.40 V, respectively. (b) A bare triangular region on the graphite surface, formed by the symmetrical adsorption of lamellae, is visible in the middle of the STM image. Image size is 23.5×23.5 nm^2. Tunneling current and voltage are 0.6 nA and −0.40 V, respectively.

To check for the influence of the spacer length (even or odd number of carbon atoms) on the molecular orientation and urea contrast, we have studied monolayers formed by $C_{12}-U-C_9-U-C_{12}$ and compared the results with $C_{12}-U-C_{12}-U-C_{12}$. Figure 6a is a large-scale STM image of a monomolecular layer of $C_{12}-U-C_9-U-C_{12}$ adsorbed from a $C_{12}-U-C_9-U-C_{12}$ solution in 1-octanol applied to the basal plane of HOPG. Figure 6b is a magnification of the middle upper area in Figure 6a. These images reveal a closely packed arrangement of $C_{12}-U-C_9-U-C_{12}$ molecules on the graphite substrate with submolecular resolution. The urea functionalities can clearly be distinguished from the remainder of the alkyl chains. The urea groups are not characterized by just one type of contrast. They appear as "bright" or "dark" rows in the STM image, similar to observations made for $C_{12}-U-C_{12}-U-C_{12}$. However, both urea rows within a lamella show the same contrast. In Figure 6c, which is a magnification of the central area in Figure 6a, as well as in Figure 6b, it is possible to observe the orientation of the molecules. The conformation of these molecules is not the same as that observed for $C_{12}-U-C_{12}-U-C_{12}$. The conformation of the molecules can be described in first approximation as bowlike. The alkyl chains are not all in line with the

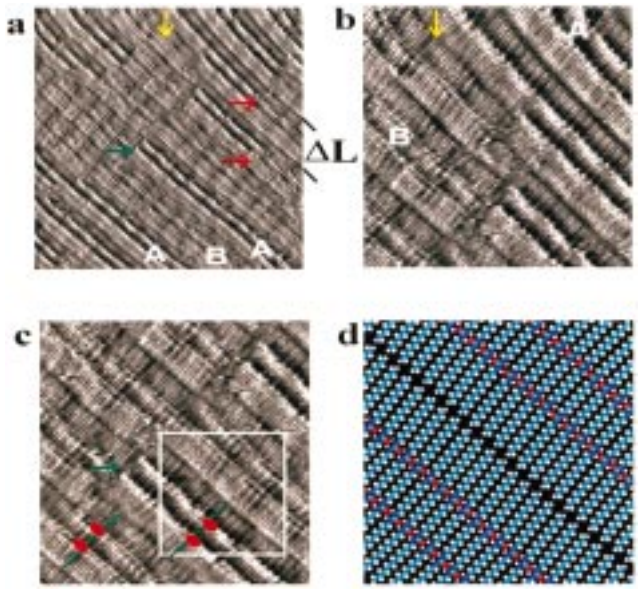

Figure 6. STM images of an ordered monolayer of $C_{12}-U-C_{12}-U-C_{12}$ molecules formed by physisorption from 1-octanol at the liquid−graphite interface. A and B in the images represent the two different lamellar types, based upon the orientation of the molecules and contrast of the urea groups (A = bright, B = dark) within the lamellae. The orientation of some molecules is indciated by a stick model. (a) A defect zone, where lamellae are shifted one-third of the lamellar width in a direction perpendicular to the lamellar axis, is indicated by a green arrow. The red arrow indicates a defect where molecules adopt a different orientation within the same row of molecules. The yellow arrow indicates the area here two lamellae, supposedly composed of monourea derivatives, are adsorbed. Image size is 30.0 × 30.0 nm^2. ΔL is the width of one lamella. Tunneling current and voltage are 1.0 nA and −0.40 V, respectively. (b) Magnification of the upper middle part of (a). Image size is 13.5 × 13.5 nm^2, representing two lamellae of probably monourea derivatives between $C_{12}-U-C_{12}-U-C_{12}$ lamellae. Tunneling current and voltage are 1.0 nA and −0.40 V, respectively. (c) Magnification of the central part of (a). Image size is 13.5 × 13.5 nm^2. The defect site where hydrogen bonding is interrupted is indicated by a green arrow. Tunneling current and voltage are 1.0 nA and −0.40 V, respectively. (d) Molecular model for the two-dimensional packing of $C_{12}-U-C_{12}-U-C_{12}$ molecules corresponding with the area indicated in (c).

substrate's symmetry axis, but the deviation from linearity is very small. The angle between the different alkyl parts is estimated to be a few degrees at maximum. Comparison with a molecular model indicates that the V-shape, which is the result of the angle formed by the $C_{12}-U-C_9$ moiety, corresponds with the direction of the carbonyl groups. A molecular model of the area indicated in Figure 6c is presented in Figure 6d. Indeed, within the same molecule or lamella, all carbonyl groups point in the same direction, contrary to $C_{12}-U-C_{12}-U-C_{12}$. In other words, also for bisurea derivatives with an odd number of carbon atoms in the alkyl spacer, not only the position but also the orientation of the urea groups can be determined. The contrast of the urea groups is related to their orientation. If we take the orientation and contrast of the molecules within the lamellae as a criterion, two types of lamellae can be distinguished, which will be called A (bright) or B (dark) type lamellae, depending on the orientation of the molecules and the contrast of the urea groups. As found for $C_{12}-U-C_{12}-U-C_{12}$, the orientation of the molecules within one lamella is not influenced by the orientation of molecules in adjacent lamellae, which can easily be seen in the large-scale STM image by the noncorrelated appearance of bright and dark lamellae. The intralamellar intermolecular distance measures 0.462 ± 0.010 nm (identical to $C_{12}-U-C_{12}-U-C_{12}$). This means that hydrogen bonding is also involved in the stabilization of the lamellae or monolayer.[21] The lamellar width is 5.0 ± 0.1 nm.

Similar to observations made for $C_{12}-U-C_{12}-U-C_{12}$, defects appear in the monolayer, for instance, in the center of the large-scale image. Frequently, lamellae are shifted by one-third of the lamellar width in a direction perpendicular to the lamellar axis. Such a defect zone is indicated with a green arrow in Figure 6a and c. At the site, indicated by the green arrow in Figure 6c, lamellae with opposite orientation of the urea groups are observed. No hydrogen bonding is possible between the molecules of both lamellae at that defect site. At the right side of this defect, a lamellar structure is formed in which the left urea row of the lower lamella is in registry with the right urea row of the upper lamella.

Another defect type, similar to $C_{12}-U-C_{12}-U-C_{12}$ monolayers, is the observation that, within one row of $C_{12}-U-C_9-U-C_{12}$ molecules, the orientation of the molecules and consequently the contrast of the urea groups is inverted. Hydrogen bonding is prohibited at this defect, which is indicated in Figure 6a by a red arrow.

In contrast with $C_{12}-U-C_{12}-U-C_{12}$, defect areas were never observed. The gaps, which are created by those lamellar shifts, are filled by molecules other than $C_{12}-U-C_9-U-C_{12}$. This is clearly shown in Figure 6b, which is the upper middle part of Figure 6a. This defect is indicated by a yellow arrow. Between lamellae, indicated as A and B, two smaller lamellae are visible which contain only one urea row. The molecular building units of those lamellae are probably some impurities (monourea derivatives).[22] Both lamellae fit perfectly in the gap created by those lateral shifts of lamellae. The contrast of the urea groups in those two small lamellae is different. The urea groups of the left lamella appear dark, while those of the right lamella appear bright. This difference in contrast is consistent with the observation that also their orientation is different as can be deduced from their conformation in the STM image. The carbonyl groups in the left lamella point to the upper left part of the image, and the carbonyl groups in the right lamella point to the lower right part. Moreover, the lamellae supposedly composed of monourea derivatives are a continuation of lamellae composed of bisurea derivatives, and the molecules are oriented in such a way that hydrogen bonding is maintained at the contact zone. This observation suggests that the orientation−contrast relation of urea groups could be a general phenomenon which holds not only for alkyl-substituted bisurea but probably also for monourea derivatives.

We have observed that, for alkyl-substituted urea derivatives, the position of the urea groups could easily be determined in the STM image. The apparent conformation of the molecules in the STM image allows identification of their orientation within the lamellae. Within a molecule, the contrast of the urea groups is identical (spacer contains an odd number of carbon atoms) or this contrast is different (spacer contains an even number of carbon atoms). Moreover, the contrast of the urea groups can be related to their orientation within the STM image. The question remains as to why a functional group can show up with different types of contrast in the same STM image.

It is known that the mismatch between the lattice of the graphite substrate and the overlayer can induce the appearance of a superstructure in the image, giving rise to a so-called Moiré pattern.[3] This contrast modulation can appear perpendicular to the lamellar boundary due to the mismatch caused by the small difference in carbon−carbon bond lengths in graphite and alkyl chains (alkanes) or along the lamellae if the position of the alkyl chains is not commensurate with the underlying graphite

substrate.[3,6,8,23] Indeed, in a lot of STM images, we find a superstructure along the lamellae, which is repeated approximately every sixth molecule. This contrast modulation is especially pronounced for the outermost alkyl chains although in some images this modulation is also visible for the urea groups. However, the contrast of both urea groups within one molecule is modulated identically. Evidently, contrast modulation along the lamellae cannot be responsible for the contrast difference found for the urea groups.

Is contrast modulation perpendicular to the lamellae responsible for the differences in contrast found for urea groups? Obviously, such a modulation can also not be responsible as the different lamellar types appear in a random way in the STM images. Moreover, the contrast of the urea groups is always related to their orientation. Finally, the lamellar axes of these compounds are not perfectly straight. Indeed, close inspection of the STM images reveals a small wavelike pattern of the lamellar axes. The period of this wavelike pattern is larger than a Moiré period. This phenomenon, which resembles the periodic offset found for 4-*n*-octyl-4′-cyanobifenyl on graphite,[24] could find its origin in a competition between the adsorbate−substrate and intermolecular interactions. Due to the strong intermolecular interactions established by hydrogen bonding, an unfavorable lattice mismatch could be relieved by the periodic lateral displacements of the molecules. However, this effect does not affect the contrast of the molecules. So, contrast modulation due to a mismatch of the overlayer with the graphite surface underneath can probably be ruled out as the responsible factor for the differences in contrast found for the urea groups.

Could sample topography come into play as a possible reason for these contrast differences? Imagine that the urea groups (or the plane made by the nitrogen atoms and the carbonyl group) are not lying parallel to the graphite surface but that the carbonyl groups point to a certain extent either toward the graphite surface or to the bulk phase. This would change the STM contrast, as any feature of the adsorbate that pushes the spatial extent of its electronic wave function farther above the surface will enhance the tunnel current associated with the adsorbate or specific functional groups of the adsorbate, in analogy with the observations reported by Cyr et al.[6] They studied the STM contrast of a terminally monosubstituted alkane bromide and observed a contrast variation of the bromine as a function of time. The bromine atoms appear bright or dark. This was attributed to a trans−gauche isomerization around the terminal C−C bond, resulting in a change in the STM image through variation in the effective spatial "overlap" between the tip and adsorbate in the tunnel junction. However, if in our system topography of the sample would play a key role in the origin of the contrast, this contrast variation should be found independently of the direction to which the carbonyl groups point within an STM image. On the contrary, the contrast and the orientation of the urea groups within an image are strongly related to each other. Therefore, topological influences of the sample can very likely be ruled out as responsible mechanism for this contrast variation although they can influence the contrast to a certain extent.

As suggested earlier, the observed effects are likely to be due to tip−adsorbate interactions. In Figure 5b, where the triangle defect is shown, the lamellae are oriented in three different ways with respect to the scan direction, and within every lamella, the urea groups show two types of contrast. However, the extent of contrast difference is affected by the relative orientation of lamellae with respect to the scan direction; i.e., the contrast difference is much less pronounced for the lamellae in the lower right corner of the STM image.

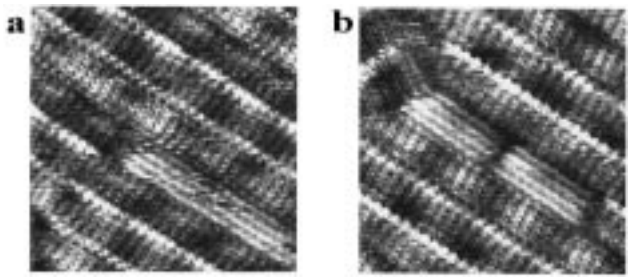

Figure 7. STM images of an ordered monolayer of $C_{12}-U-C_{12}-U-C_{12}$ molecules formed by physisorption from 1-octanol at the liquid−graphite interface, taken immediately after each other. The only difference between the experimental conditions applied for the acquisition of both STM images is a sample rotation of 180°. Image size of (a) and (b) is 10×10 nm^2. Tunneling current and voltage are 1.0 nA and −0.53 V, respectively. These images have been taken at a defect site of the monolayer in order to be able to compare both images. The images do not match perfectly due to sample drift. In fact, the contrast of the urea groups is not substantially affected by rotation. The brighter row of urea groups remains the brightest one after sample rotation.

Although sometimes the contrast difference seems to be independent of the scan direction, as shown in Figure 7, these observations cannot be generalized. In some pictures, the contrast difference shows up as a distinct difference in the "brightness" of the urea groups (Figures 5−7). In other pictures, the contrast difference is determined by a more subtle difference in the sequence of bright and dark spots (Figure 3). Sometimes, the contrast difference is very weak or not visible at all. In general terms, the degree of the contrast difference is not only affected by the orientation of the lamellae with respect to the scan direction but also depends strongly on the condition of the tip. It should be mentioned that the same phenomena appear in topography images. Therefore, we suggest that specific tip−adsorbate interactions determine the contrast of the urea groups and that the tip shape plays a key role in the contrast of the urea groups.

Conclusions

In this paper, we have compared the two-dimensional packing of physisorbed monolayers of alkylated bisurea derivatives, which were imaged with submolecular resolution at the liquid−graphite interface. The position of the urea moieties could clearly be determined in the STM images. The apparent conformation of the molecules in the STM images allowed the molecular orientation and, consequently, the orientation of the functional groups to be determined. It was shown that the conformation of the molecules depends on the number of carbon atoms in the alkyl spacer, resulting in an odd−even effect. Intralamellar hydrogen bonding stabilizes the lamellar structures and monolayer defects could be imaged with high resolution, even allowing the imaging of isolated lamellae with submolecular resolution.

Besides this clear structural identifiability of the system, another phenomenon was observed which, to our knowledge, was not reported before. In some STM images, the contrast of both urea groups in one molecule is identical if the alkyl spacer contains an odd number of carbon atoms, while the contrast of the urea groups is different if the alkyl spacer contains an even number of carbon atoms. Moreover, the urea groups can appear with two different types of contrast in the same STM image and the contrast of the urea groups is related to their orientation. This orientation−contrast relation allows the determination of

the molecular orientation of whichever molecule in parallel lamellae within the same STM image, once this relation is established.

We have shown for this particular class of compounds that it is possible to differentiate between two formally equivalent functional groups within a molecule, not only on the basis of their difference in position but also on the basis of their contrast, which is correlated with the orientation.

We have ruled out lattice mismatch of the monolayer with respect to the graphite surface and topological factors as responsible mechanisms for the observed contrast difference of the urea groups. It is very likely that tip−adsorbate interactions are responsible for the observed phenomena.

Acknowledgment. The authors thank FWO and DWTC for continuing financial support through IUAP-IV-11. S.D.F. is a predoctoral fellow of the Fonds voor Wetenschappelijk Onderzoek. This research was supported by the "Stichting Technische Wetenschappen" (STW) and the Dutch Foundation for Scientific Research (NOW) (J.v.E, R.M.K., B.L.F.).

References and Notes

(1) McGonigal, G. C.; Bernhardt, R. H.; Thomson, D. J. *J. Appl. Phys. Lett.* **1990**, *57*, 28.

(2) McGonigal, G. C.; Bernhardt, R. H.; Yeo, Y. H.; Thomson, D. J. *J. Vac. Sci. Techol*. **1991**, *B9*, 1107.

(3) Rabe, J. P.; Buchholz, S. *Science* **1991**, *253*, 424.

(4) Venkataraman, B.; Breen, J. J.; Flynn, G. W. *J. Phys. Chem*. **1995**, *99*, 6608.

(5) Watel, G.; Thibaudau, F.; Cousty, J. *Surf. Sci*. **1993**, *281*, L297.

(6) Cyr, D. M.; Venkataraman, B.; Flynn, G. W.; Black, A.; Whitesides, G. M. *J. Phys. Chem.* **1996**, *100*, 13747.

(7) Venkataraman, B.; Breen, J. J.; Flynn, G. W.; Wilbur, J. L.; Folkers, J. P.; Whitesides, G. M. *J. Phys. Chem*. **1995**, *99*, 6608.

(8) Hibino, M.; Sumi, A.; Hatta, I. *Jpn. J. Appl. Phys*. **1995**, *34*, 3354.

(9) Eigler, D. M.; Weiss, P. S.; Schweizer, E. K.; Lang, N. D. *Phys. Rev. Lett*. **1991**, *66*, 1189.

(10) Mizutani, W.; Shigeno, M.; Ono, M.; Kajimura, K. *Appl. Phys. Lett*. **1990**, *56*, 1974.

(11) Morozov, V. N.; Seeman, N. C.; Kallenbach, N. R. *Scanning Microsc*. **1993**, *7*, 757.

(12) Lindsay, S. M.; Sankey, O. F.; Li, Y.; C., H.; Rupprecht, A. *J. Phys. Chem*. **1990**, *94*, 4655.

(13) Spong, J. K.; Mizes, H. A.; LaComb, L. J., Jr.; Dovek, M. M.; Frommer, J. E.; Foster, J. S. *Nature* **1989**, *338*, 137.

(14) Foster, J.; Frommer, J. *Nature* **1988**, *333*, 542.

(15) Claypool, C. L.; Faglioni, F.; Goddard, W. A., III; Gray, H. B.; Lewis, N. S.; Marcus, R. A. *J. Phys. Chem. B* **1997**, *101*, 5978.

(16) Faglioni, F.; Claypool, C. L.; Lewis, N. S.; Goddard, W. A., III *J. Phys. Chem. B* **1997**, *101*, 5996.

(17) For an excellent review, see: Cyr. D. M.; Venkataraman, B.; Flynn, G. W. *Chem. Mater*. **1996**, *8*, 1600.

(18) Vanoppen, P.; Grim, P. C. M.; Rücker, M.; De Feyter, S.; Moessner, G.; Valiyaveettil, S.; Müllen, K.; De Schryver, F. C. *J. Phys. Chem.* **1996**, *100*, 19636.

(19) Grim, P. C. M.; De Feyter, S.; Gesquière, A.; Vanoppen, P.; Rücker, M.; Valiyaveettil, S.; Moessner, G.; Müllen, K.; De Schryver, F. C. *Angew. Chem., Int. Ed. Engl.* **1997**, *36*, 2601.

(20) van Esch, J.; De Feyter, S.; Kellogg, R. M.; De Schryver, F.; Feringa, B. L. *Chem. Eur. J.* **1997**, *3*, 1238.

(21) The precise determination of the intermolecular distance is possible due to the appearance of a Moiré pattern along the lamellar axis. The intermolecular distance was determined from a number of larger scale STM images which exhibit a pronounced Moiré pattern. Examination of 28 crystal structures of noncyclic urea compounds deposited in the Cambridge Crystallographic Database revealed that the average distance between two successive hydrogen-bonded urea groups is 0.46 nm.

(22) This impurity could be 1,3-bisdodecylurea.

(23) Cincotti, S.; Rabe, J. P. *Appl. Phys. Lett.* **1993**, *62*, 3531.

(24) Frommer, J. *Angew. Chem., Int. Ed. Engl.* **1992**, *31*, 1298.